MODEL OF ULTRASONIC RAY PATHS IN AN ANISOTROPIC WELD BASED ON RAY METHOD

Q. Liu, H. Wirdelius
Chalmers Lindholmen University College, Göteborg, Sweden

Abstract: Experiences from isotropic materials suggest that it is impossible to derive a statistical model with few parameters to model a weld in an anisotropic material. The parameter that remains unknown even after a large number of empirical investigations is the orientation of the dendrites due to the heating. Our intention is to apply some simplified models in an optimization scheme to predict the dendrites' orientation in different kinds of welds. In this paper, a model of ultrasonic ray traveling through anisotropic materials, as well as the corresponding computer simulation is presented.
First, based on the previous work on texture analysis of various austenitic stainless steel weld samples, a typical simplified model of the geometry of welds is established. It is subdivided into a finite number of smaller regions with specific anisotropy. Then by means of the ray tracing method, ray path running through the weld model is developed. As a function of incident angle, the point of entrance of the sound path to the weld and the given orientation of the dendrites, the model will ultimately give the point where the sound leaves the weld, the time of flight and the angle between the sound ray and the weld.
A numerical simulation of the forward problem is also provided as a validation of the model.

Introduction: Non destructive testing (NDT) is a commonly used industrial method to evaluate the integrity of individual components. In-service induced cracks such as fatigue and stress corrosion cracks can, if they are detected, be sized and monitored in order to postpone repairs or replacements. The reliability of a NDT method is highly dependent on how the equipment is adjusted to a specific object and to anticipated crack features. If ultrasonic NDT is applied on materials with strong anisotropy (e.g. welds in stainless steel) it can introduce possible difficulties in the interpretation as the ultrasound tends to bend in an unpredicted way. Ultrasonic NDT techniques to size defects are mainly based on the information of ultrasound paths from the crack tips and thus very sensitive to these kind of effects.
According to the Swedish Nuclear Power Inspectorate's requirements in the regulations concerning structural components in nuclear installations, in-service inspection must be performed using inspection methods that have been qualified. These demands on reliability of used NDE/NDT procedures and methods have stimulated the development of simulation tools of NDT. Experiences done by modeling and verification towards isotropic materials suggest that it is not possible to derive a statistical model with few parameters to model a weld in an anisotropic matrix material. The parameter that remains unknown even after a large number of empirical investigations is the orientation of the dendrites due to the heating. This is also probably the most important parameter in determining the sound path through the weld.
Numerical methods based on discretization of the simulated volume (e.g. finite element methods and EFIT [1]) are well suited to model objects with complex material structure. Since the number of elements to ensure accuracy in this kind of methods soon increases to an unmanageable amount, simulation has in general been limited to two-dimensional configurations ([2], [3]). Exact methods have been applied to less compound structures (layered anisotropy), though full three-dimensional objects including crack scattering ([4]). The solidification process is individual for each weld and the resulting dendrite orientation (and anisotropy) can only be assumed to be homogenous in small fractions of the volume. It is therefore difficult to find simple functions to describe the distribution of the orientation. Ray tracing techniques based on high frequency approximations have been applied to model three-dimensional welded volumes ([5], [6], [7] and [8]). Often these utilize subdivision of the volume in homogenous parts or descriptions of the orientation by functions based on ad hoc assumptions of the solidification process.

The present paper gives a short description of a simple ray tracing model of ultrasonic propagation through a welded region. This paper is the first part in a project that will develop an ultrasonic technique to retrieve the anisotropy directivity in a welded region. This model together with experimental data is to be implemented in an optimization algorithm to calculate the orientation of the dendrites in the real weld. The final application has enforced the simplicity and reduced the number of possible parameters within the model. The paper initially starts of with a declaration and justification of the model being limited to represent transversely isotropy material. Thereafter a simplified model of the geometry of welds is deduced. This is based on the previous work on texture analysis of various austenitic stainless steel weld samples and also subdivides the volume in a finite number of smaller regions with homogeneous anisotropy. The ray tracing model is subsequently presented and the paper also includes a minor numerical example.

Elastic anisotropy in stainless steel weld: A material can be stated to be anisotropic if its properties, when measured at the same location, change with direction.
The simplest anisotropic case of broad engineering applicability is transversely isotropy, which has one distinct direction, while the other two directions are equivalent to each other which form an isotropic plane.
Earlier works on both the application of ultrasonic NDT and the destructive examination of welds have shown that the austenitic stainless steel weld can be modeled as transversely isotropy, due to the ordered columnar structure, similar to a fiber texture. That is to say, around some principal direction, there is a random angular orientation of the crystals. Thus, in a plane perpendicular to these preferred directions the material is assumed to be isotropic.
Due to this kind of structural symmetry, the elastic modulus matrix thus has five independent components among twelve nonzero components, giving the elastic modulus matrix the form ([9])

$$C = \begin{bmatrix} c_{11} & c_{12} & c_{13} & 0 & 0 & 0 \\ c_{12} & c_{11} & c_{13} & 0 & 0 & 0 \\ c_{13} & c_{13} & c_{33} & 0 & 0 & 0 \\ 0 & 0 & 0 & c_{44} & 0 & 0 \\ 0 & 0 & 0 & 0 & c_{44} & 0 \\ 0 & 0 & 0 & 0 & 0 & c_{66} \end{bmatrix} \tag{1}$$

where, $c_{66} = (c_{11} - c_{12})/2$ and the third direction is taken as the principal axis.

Model of the geometry of a typical weld: The extensive columnar grain structure in austenitic welds differs greatly from that in ferritic welds. In both cases, the solidification process during welding initially produces a columnar grain structure in each weld bead. Grains grow along the maximum thermal gradients in the bead ([10]). Growth in one particular direction is faster than in other directions and this leads to the rapid disappearance of out-of-plane oriented grains. In the following, the deposition of subsequent weld metal reheats the beads partially and, in the case of a ferritic weld, the columnar grain structure is destroyed by the austenite-ferrite phase transformation that occurs as the solid cools. No such transition occurs in the austenitic alloys and consequently the columnar grain structure survives. Furthermore, each new weld bead re-melts the surface of the preceding beads and the new grains grow epitaxially on the existing ones. Consequently grains of substantial length are produced. In Fig.1, a macrograph of a typical V-butt weld is shown.

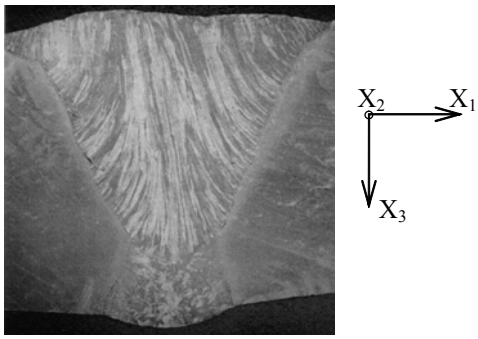

Fig.1 Macrograph of an austenitic stainless steel weld

Seen from the picture, apparently, the crystalline structure is composed of a series of long grains, whose dendrite directions are spatially varied. The columnar structure of the austenitic weld shows that the long columnar dendrites begins at the fusion lines and extends into the body of the weld. What's more, the long dendrite axis is almost vertical along the centre of the weld and nearly perpendicular to the fusion lines and the upper boundary of the weld. This presents the possibility of modeling the dendrite directions, in a primitive assumption of the structure, with the following expression

$$X_3^i = a_1^i \left(X_1^i - X_1^{bi} \right)^{a_2^i} \tag{2}$$

where, a_1^i, a_2^i, X_1^{bi} are defined by the geometric relation at the fusion line and upper boundary. The values of these coefficients may be changed according to certain assumption made to the structure of a specific weld.

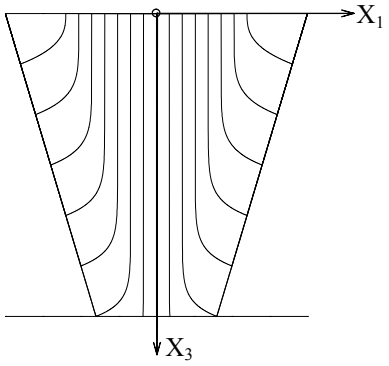

Fig.2 Plot of the weld model

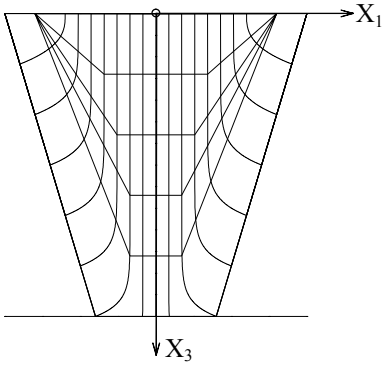

Fig.3 Plot of the sub-regions in a weld model

Equation (2) is utilized to define the boundaries of the dendrite orientations in Fig. 1 and an example of this is visualized in Fig. 2. The regions outside are modeled as ferritic materials and are assumed to have homogeneous and isotropic elasticity properties (almost certainly true compared with the welded region).

According to the requirement of modeling and simulation, the whole weld is thereafter subdivided into smaller regions with predefined homogeneous transversely anisotropy (Fig. 3). The directivity in each fraction is given by the mean value of that provided by the centre of its boundaries. The elastic property in each fraction is assumed almost the same and then can be regarded as homogeneous transversely isotropy.

Ray tracing model: In order to simulate an ultrasound wave propagating through a weld, a mathematical model is established here. In this paper, we only consider the propagating direction of a quasi P-wave (also called longitudinal wave). No information about the amplitude of rays is

deduced and the analysis is limited to the quasi P-wave mode. The model comprises mainly the following parts.

1. Expression of the phase velocity as a function of the phase angle

Unlike the wave propagation in isotropic medium, the phase velocity of quasi P-wave in anisotropic material on the other hand is a function of the angle between the wave normal direction and the long axis of the columnar grains.

For a general elastic anisotropic medium, in the absence of body forces, the wave equation may be written in the form ([11]),

$$\rho \ddot{u}_i = \sigma_{ij,j} \tag{3}$$

where u_i is the displacement vector, ρ is the density and σ_{ij} is the stress tensor. The summation convention is used, dot represents partial time differentiation and a Cartesian coordinate system (x_1, x_2, x_3) has been introduced. The stress tensor σ_{ij}, by means of Hooke's law, may be written as,

$$\sigma_{ij} = C_{ijkl}\varepsilon_{kl} \quad \text{where } \varepsilon_{ij} = \left(u_{i,j} + u_{j,i}\right)/2 \tag{4}$$

ε_{ij} is the linear strain tensor and C_{ijkl} is the stiffness tensor.

Assume a plane wave propagating in $\mathbf{x}_1\mathbf{x}_3$-plane,

$$\mathbf{u} = \left(u_1\mathbf{x}_1 + u_2\mathbf{x}_2 + u_3\mathbf{x}_3\right)e^{ik\left(l_1\mathbf{x}_1 + l_3\mathbf{x}_3 - vt\right)} \tag{5}$$

where k is the wave number, l_i is related to traveling angle and v is the velocity of the wave. The consistence of $\mathbf{x}_1\mathbf{x}_3$-system with the crystal coordinate system is supposed.

The combination of equations (3)-(5) gives the Christoffel equation,

$$\begin{bmatrix} A-\rho v^2 & \alpha & \beta \\ \alpha & B-\rho v^2 & \gamma \\ \beta & \gamma & C-\rho v^2 \end{bmatrix}\begin{bmatrix} u_1 \\ u_2 \\ u_3 \end{bmatrix} = 0 \tag{6}$$

For an anisotropic medium, with $\mathbf{x}_3$ as the principal crystal axis of the columnar grain,

$$\begin{aligned} A &= c_{11}l_1^2 + c_{44}l_3^2 \\ B &= c_{66}l_1^2 + c_{44}l_3^2 \\ C &= c_{44}l_1^2 + c_{33}l_3^2 \\ \beta &= \left(c_{13} + c_{44}\right)l_1 l_3 \\ \alpha &= \gamma = 0 \end{aligned}$$

From the condition for the existence of a non-trivial solution, there must be

$$\begin{vmatrix} A-\rho v^2 & \alpha & \beta \\ \alpha & B-\rho v^2 & \gamma \\ \beta & \gamma & C-\rho v^2 \end{vmatrix} = 0 \tag{7}$$

Solution of above expression gives the velocity of a quasi P-wave as,

$$v_p^2 = \mu^2 \left[1 - \lambda + \varepsilon \sin^2\theta + \sqrt{\Delta_1 \sin^4\theta + \Delta_2 \sin^2\theta + \Delta_3} \right] \tag{8}$$

where, $\mu, \lambda, \varepsilon, \Delta_1, \Delta_2, \Delta_3$ are coefficients relating to the elements of stiffness matrix. The equation above clearly clarifies the relationship between the phase velocity and the corresponding phase angle.

2. Relationship between phase angle and ray angle

The velocity of principal interest in ultrasound propagating is the group (or ray) velocity. Since in anisotropic material the phase velocity of longitudinal waves is a function of the angle between the wave normal and the principal axis of the columnar grains, the group velocity in general does not have the same direction and magnitude. Referring to Fig.4, the ray direction can be expressed with its components

$$\tan\theta_g = \frac{\partial\omega}{\partial k_1} \Big/ \frac{\partial\omega}{\partial k_3} \tag{9}$$

where,

$$\left.\frac{\partial\omega}{\partial k_1}\right|_{k_3=const} = \left.\frac{\partial(kv)}{\partial k_1}\right|_{k_3=const} = \left.\left(v\frac{\partial k}{\partial k_1} + k\frac{\partial v}{\partial k_1} \right)\right|_{k_3=const} = \left.\left(v\frac{\partial k}{\partial k_1} + k\frac{\partial v}{\partial\theta}\frac{\partial\theta}{\partial k_1} \right)\right|_{k_3=const} \tag{10}$$

When $k_3 = const$, further derivation gives $\partial\theta/\partial k_1 = \cos\theta/k$ and $\partial k/\partial k_1 = \sin\theta$. If they are substituted in equation (10), it becomes,

$$\left.\frac{\partial\omega}{\partial k_1}\right|_{k_3=const} = v\sin\theta + \frac{dv}{d\theta}\cos\theta$$

In a similar way, the following expression can be achieved,

$$\left.\frac{\partial\omega}{\partial k_3}\right|_{k_1=const} = v\cos\theta - \frac{dv}{d\theta}\sin\theta$$

Thus the relationship between ray angle and phase angle is,

$$\tan\theta_g = \frac{\partial\omega}{\partial k_1} \Big/ \frac{\partial\omega}{\partial k_3} = \left(v\sin\theta + \frac{dv}{d\theta}\cos\theta \right) \Big/ \left(v\cos\theta - \frac{dv}{d\theta}\sin\theta \right) \tag{11}$$

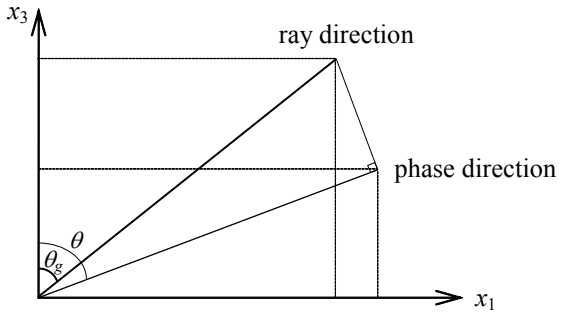

Fig.4 Relationship between ray direction and phase direction

3. Determination of the direction of the phase velocity for a set ray

Considering the ultrasonic wave running in a layered structure, if a ray direction in the anisotropic medium is set, the corresponding phase direction is essential to be retrieved so that proper boundary condition between two adjacent media can be utilized.

Based on the equations (8) and (11) presented above, the following equation can be reached, from which the correct phase angle is obtained.

$$y^6 + a_5 y^5 + a_4 y^4 + a_3 y^3 + a_2 y^2 + a_1 y + a_0 = 0 \tag{12}$$

where, $y = \sin^2\theta$ and a_i are coefficients. The effect of ray direction exists in an implicit way in the coefficients of the equation.

4. The phase angle of the transmitted P-wave

Snell's law is widely used in ultrasonic testing to calculate the angle of refracted beams. According to Snell's law, incident and refracted waves all lie in the same plane and they must have the same component of the wave vector tangential to the interface. Since the slowness surface is the inverse of the phase velocity, as a function of the wave vector direction, Snell's law can certainly be used to the slowness surface.

In the incident medium, the projection of slowness to the boundary at a certain angle is $s_1 = m \cdot \sin\theta$, in which, the slowness is $m = \left(1/v_p\right)$. This represents one side of Snell's law.

The other side of Snell's law surely is the projection of slowness in medium 2. Therefore Snell's law states that the boundary condition is

$$s_1 = s_2 = m' \cdot \sin\theta' \tag{13}$$

This introduces another equation for solving the phase angle of the transmitted quasi P-wave,

$$y^4 + b_3 y^3 + b_2 y^2 + b_1 y + b_0 = 0 \tag{14}$$

here, $y = \sin^2\theta'$ and θ' is the phase angle of the transmitted quasi P-wave.

Apparently, this approach provides a valid means to calculate the refracted ray angle in anisotropic medium, while it says nothing about the information on the amplitude of the refracted wave.

In practical operation, some certain coordinate transformation can be necessary so as to acquire the correct coefficients b_i in equation (14). What is more, a criterion for choosing the most suitable root is inevitable.

5. Determination of the ray angle of the transmitted P-wave

The ray angle of a transmitted wave can easily be achieved with equation (11), if we know the expression of phase velocity as well as the phase angle. In this paper, we supply another approach in order to provide some more intuitive insight of the physical phenomenon of the wave propagating in an anisotropic medium.

Under the assumption of the slowness surface being known in one anisotropic medium, the ray direction at one point is exactly the gradient of the slowness iso-value surface at that point. Suppose in a polar coordinate system, the iso-value surface of slowness is $M\left(r,\theta\right)$, then the gradient of this surface is,

$$\nabla M(r,\theta) = \mathbf{r}\frac{\partial M}{\partial r} + \boldsymbol{\theta}\frac{1}{r}\frac{\partial M}{\partial \theta} \tag{15}$$

The ray direction in our boundary Cartesian coordinate system (referring to Fig. 4) then may be calculated with the definition of dot product of two vectors, that is,

$$\cos\theta_g = \frac{\nabla M}{\left|\nabla M\right|} \cdot \mathbf{x}_3 \tag{16}$$

It is easy to show that both these two methods are equivalent.

Generally, with these five principal parts of the model, the propagating direction of a transmitted P-wave caused by an incident P-wave can be determined. Although the present approach is applied to quasi P-wave transmission, it is also appropriate for the ray tracing of shear waves.

Numerical example: A numerical example of a quasi P-wave traveling through two anisotropic half spaces is presented here.
As shown in Fig. 5, an anisotropic medium 1 occupies the lower half space, with a crystal axis of 80° counter-clockwise to $\mathbf{x}_3$. A quasi P-wave with an incident angle of 120° to the principal crystal axis impinges the boundary.
The simulation steps include the determination of the phase angle in medium 1, the wave number in horizontal direction and the calculation of transmitted ray's direction.
In order to validate the model, the medium 2 in upper half space is set to have the same crystal axis direction as that in lower half space. The output shows the transmitted quasi P-wave ray propagates in the upper half space with an angle of 40° to $\mathbf{x}_3$. The corresponding phase angle is about 33.58° to $\mathbf{x}_3$. The geometry relationship exhibits the validity of the model.

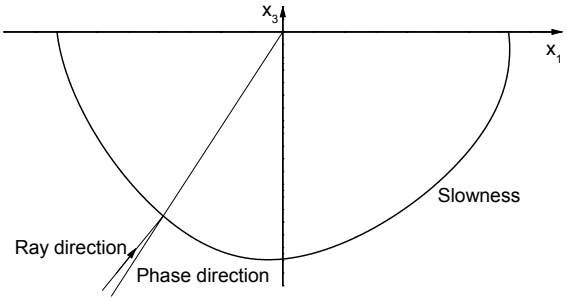

Fig. 5 Diagram of wave traveling in medium 1

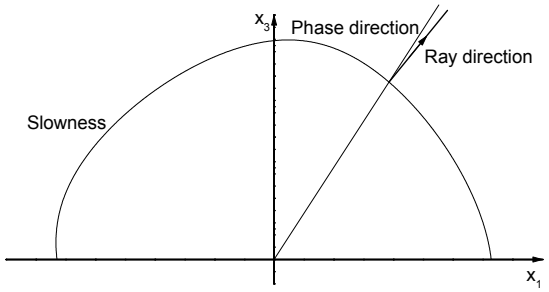

Fig. 6 Diagram of wave traveling in medium 2

Conclusion and future plan: The present model solves the forward problem and can be utilized as a ray tracing method simulating the ultrasonic path in an anisotropic weld. The similar method can also be applied in other engineering area ([12], [13]).The included example is for a quasi P-wave but the model is of course also valid to model the propagation of quasi shear waves. The deduced model is to be used in an optimization scheme to solve the inverse problem. The model will be applied in the development of an ultrasonic technique (phased array) to retrieve the anisotropy directivity in a welded region. The final application has enforced the simplicity and reduced the number of possible parameters within the model.

References:

[1] P. Fellinger, R. Marklein, K.J. Langenberg and S. Klaholz, "Numerical modelling of elastic wave propa-gation and scattering with EFIT-Elastodynamic Finite Integration Technique, Wave Motion 21, pp. 47-66, 1995.

[2] K.J. Langenberg, R. Hannemann, T. Kaczorowski, R. Marklein, B. Koehler, C. Schurig and F. Walte, "App-lication of modeling techniques for ultrasonic austenitic weld inspection", NDT&E International 33, pp. 465-480, 2000.

[3] S. Halkjær, M.P. Sørensen and W.D. Kristensen, "The propagation of ultrasound in an austenitic weld", Ultrasonic 38, pp. 256-261, 2000.

[4] A.S. Eriksson, J. Mattsson and A.J. Niklasson, "Modelling of ultrasonic crack detection in anisotropic materials", NDT&E International 33, pp. 441-451, 2000.

[5] J.A. Ogilvy, "A model for elastic wave propagation in anisotropic media with applications to ultrasonic inspection through austenitic steel", British Journal of NDT 27:1, pp. 13-21, 1985.

[6] J.A. Ogilvy, "Computerized ultrasonic ray tracing in austenitic steel", NDT International 18:2, pp. 67-77, 1985.

[7] V. Schmitz, F. Walte and S.V. Chakhlov, "3D ray tracing in austenitic materials", NDT&E International 32, pp. 201-213, 1999.

[8] A. Lhémery, P. Calmon, I. Lecæur-Taïbi, R. Raillon and L. Paradis, "Modeling tools for ultrasonic inspect-tion of welds", NDT&E International 33, pp. 499-513, 2000.

[9] B.A. Auld, "Acoustic fields and waves in solids", Robert E. Krieger Publishing Company, 1990.

[10] J.R. Tomlinson, A.R. Wagg and M.J. Whittle, "Ultrasonic inspection of austenitic welds", British Journal of NDT, pp.119-127, 1980.

[11] J.D. Achenbach, "Wave propagation in elastic solids", North-Holland, 1975.

[12] M.A. Slawinski, "On elastic-wave propagation in anisotropic media: reflection/refraction laws, raytracing and traveltime inversion", Ph.D. thesis, the University of Calgary, 1996.

[13] L. Thomsen, "Weak elastic anisotropy", Geophysics 51:10, pp. 1954-1966, 1986.